Journal of Applied Polymer Science

Deposition of calcium hydroxyapatite on negatively charged polyphosphazene surfaces

Tomasz Modzelewski, Ian Hotham, Harry R. Allcock
Department of Chemistry, the Pennsylvania State University, University Park, Pennsylvania 16802
Correspondence to: H. R. Allcock (E-mail: hra@chem.psu.edu)

ABSTRACT: A number of polyphosphazenes with negatively charged β-alanine (β-Ala) and γ-amino butyric acid (GABA) side groups were synthesized and studied for their ability to initiate the growth of hydroxyapatite (HAp) during exposure to simulated body fluid (SBF). All the polymers were hydrolytically sensitive, with the final hydrolysis rate dependent on the specific active side groups (GABA > β-Ala). These systems also underwent extensive mineralization, with calcium phosphate deposited across their entire surface during exposure to SBF (up to 115 wt % gain after 4 weeks). This degree of deposition is a major advance over previously reported polyphosphazene systems, which underwent a maximum of 27 wt % gain after immersion in SBF for 4 weeks. The extent of mineralization over the surface was monitored using environmental scanning electron microscopy (ESEM) coupled with energy dispersive X-ray spectroscopy (EDS). In addition, X-ray diffraction (XRD) was used to determine the identity of the mineralized material. © 2014 Wiley Periodicals, Inc. J. Appl. Polym. Sci. **2015**, *132*, 41741.

KEYWORDS: biodegradable; biomedical applications; biomimetic

Received 5 September 2014; accepted 11 November 2014
DOI: 10.1002/app.41741

INTRODUCTION

More than 2.2 million bone graft procedures are performed worldwide each year, with autografts and allografts used to treat most cases.[1,2] However, due to the drawbacks associated with these procedures, the use of synthetic polymeric tissue engineering scaffolds would be a major advance in the field.[3] In the tissue engineering approach, a biodegradable three-dimentional scaffold is utilized as a foundation to carry signaling motifs to enhance cellular response and facilitate infiltration by new tissue as the injury site heals.[4]

Earlier investigations into the development of scaffolding materials have focused on the use of synthetic organic polymers (e.g., polylactic or polylactic-*co*-glycolic acid) which are capable of mimicking the physical properties of bone, primarily its load bearing capability.[5–7] However, these polymers hydrolyze to acidic products that can lower the local pH and lead to a decrease in tissue ingrowth and, in extreme cases, to tissue necrosis.[6,8,9] Polymers derived from living things, such as chitosan, have also been studied extensively due to their enhanced cellular adhesion and recognition.[10] However, most of these naturally derived polymers have poor mechanical properties that make them unsuitable for load bearing applications.[11] Furthermore, the polymer backbone is susceptible to enzymatic attack which makes the rate of hydrolytic breakdown unpredictable.[12]

In an attempt to mimic the composite nature of bone, macromolecules have also been functionalized with acidic (carboxylate and phosphonate) groups to facilitate the binding of calcium and to nucleate the growth of hydroxyapatite (HAp) to better mimic the composite structure of the parent tissue.[10,13–16] However, as these systems generally use the above mentioned polymers, they also suffer from the drawbacks associated with those samples.

In the current study, polyphosphazenes were synthesized with negatively charged γ-amino butyric acid (GABA) and β-alanine (β-Ala) side groups designed to coordinate calcium ions and allow the deposition of HAp during exposure to a simulated body fluid (SBF) solution. Polyorganophosphazenes are hybrid inorganic/organic polymers with an alternating nitrogen and phosphorus backbone, with each phosphorus atom functionalized with two organic side groups which govern the chemical and physical properties of the final material.[17,18] Previous work has shown that polyphosphazenes with biologically compatible side groups are biocompatible,[19,20] have highly tunable rates of hydrolytic breakdown[21] and are capable of producing a minimal inflammatory response when implanted *in vivo*.[19,22] More recently, we have investigated polyphosphazenes containing phosphonic acid functionalized side groups, in an attempt to generate materials capable of nucleating the growth of hydroxyapatite during

Additional Supporting Information may be found in the online version of this article.

exposure to SBF.[23,24] Although these materials were shown to have hydroxyapatite deposits on their surface, the coatings were sparse, with very little HAp deposited during the 4 week trial. In this work, we shifted the focus toward maximizing the acidic content of the polymers in order to optimize their potential to coordinate calcium ions from solution and facilitate the growth of hydroxyapatite over the entire surface. The new polymers were shown to be biodegradable and possess the ability to grow significant amounts of hydroxyapatite uniformly across the entire surface when exposed to SBF.

EXPERIMENTAL

Reagents and Equipment for Polymer Synthesis and Characterization

Information is provided in the Supporting Information.

Esterification of Asp, Glu, β-Alanine, and γ-Amino Butyric Acid

The synthetic protocol and characterization data are provided in the Supporting Information.

Synthesis of Allyl Ester Protected Polymers

The synthesis of polymers **2**-**5** followed a similar procedure, with a representative example given for polymer **2**. Poly(dichlorophosphazene) (3.00 g, 25.9 mmol) was dissolved in tetrahydrofuran (THF) (300 mL). In a separate vessel, *p*-cresol (1.67 g, 15.5 mmol) was added to a suspension of sodium hydride (NaH) (60% w/w) (0.52 g, 13.0 mmol) in THF (200 mL). Once the NaH was consumed, the sodium aryloxide salt was added slowly to the polymer solution and the mixture was stirred at 25°C for 24 h. Progress of the reaction was monitored by ^{31}P NMR spectroscopy. In a separate vessel, triethylamine (TEA) (26.2 g, 259 mmol) was added to a suspension of β-alanine allyl ester hydrochloride (17.2 g, 104 mmol) in THF (200 mL) and the mixture was refluxed for 4 h before being transferred to the polymer solution via filter addition. The resulting solution was then refluxed for an additional 48 h. Once the substitution was complete, the polymer solution was concentrated under reduced pressure and precipitated twice into water from THF before drying under high vacuum to afford the product as a white solid. The characterization data are provided in Table I. (Note: During the synthesis of polymers **4** and **5**, neither the amino-containing reactant nor the polymer solutions were refluxed. The polymer solutions were heated to ~50°C and stirred for 72 h. after amine addition which was sufficient to obtain complete chlorine replacement).

Deprotection of Allyl Ester Units

The de-esterification of the polymers followed an adopted literature procedure.[25] The characterization data are provided in Table I.

Deprotection of 75% Amino-Bearing Polymers 2 and 4

A representative example is given for polymer **2**. To a solution of **2** (3.00 g, 10.3 mmol) in THF (600 mL) was added morpholine (8.97 g, 103 mmol) and $Pd(PPh_3)_4$ (0.119 g, 0.103 mmol). The resulting solution was stirred for 1 h. at room temperature, during which time the polymer precipitated as a fine powder. Methanol (100 mL) was added to the suspension, causing the powder to collect into a single mass. The solid sample was purified in a Soxhlet extractor for 2 days using THF to remove any remaining palladium. The product was then dried under high vacuum to afford the final polymer as a brittle, off-white solid with <10 mol % allyl ester groups remaining as determined by ^{1}H NMR.

Deprotection of 50% Amino Group Polymers 3 and 5

A representative example is provided for polymer **3**. To a solution of polymer **3** (2.00 g, 7.14 mmol) in THF (500 mL) was added morpholine (6.18 mL, 71.4 mmol) and $Pd(PPh_3)_4$ (0.205 g, 0.179 mmol). This solution was stirred for 1 h at 25°C before concentration of the sample under reduced pressure and dialysis against methanol:dichloromethane (1 : 1) for 3 days. The solvent was then removed under reduced pressure to give the final polymer as an off-white solid. The complete removal of allyl ester groups was confirmed by ^{1}H NMR.

Hydrolysis of Polymers 3a and 5a

Polymer films were cast using 20 mL of a 5% w/v solutions of the polymers in a 1 : 1 mixture of chloroform:methanol in Teflon-coated boats (25 cm^2). The solvent was allowed to evaporate slowly at 25°C. The films were then dried further under high vacuum for an additional 48 h. The films were cut into 10 mg^2 (1 cm^2) and were immersed in 5 mL of TRIS buffered saline (50 m*M* TRIS, 150 m*M* NaCl) at pH = 7.35 and maintained at 37°C. Three samples were removed every week for 6 weeks, dried under vacuum and reweighed to determine film mass loss. The data are summarized in Figure 2(a).

Preparation of 1.5X Simulated Body Fluid

The 1.5X SBF solution was prepared according to a previously reported procedure.[26] Specifically, NaCl, $NaHCO_3$, KCl, $K_2HPO_4{\cdot}3H_2O$, $MgCl_2{\cdot}6H_2O$, 1M HCl, $CaCl_2$, Na_2SO_4 and TRIS were added sequentially to deionized water, with additional 1M HCl added to adjust the pH to 7.35. Final ion concentrations in solution were: Na^+ (213.0 m*M*), K^+ (7.5 m*M*), Mg^{2+} (2.3 m*M*), Ca^{2+} (3.8 m*M*), Cl^- (221.7 m*M*), HCO_3^- (6.3 m*M*), HPO_4^{2-} (1.5 m*M*), SO_4^{2-} (0.75 m*M*).

Mineralization of Polymer 3a and 5a

Polymer films, cast by the above described procedure were dried and cut into 50mg squares (5 cm^2), immersed in 15 mL of 1.5X SBF[27,28] at pH = 7.35, agitated, and maintained at 37°C. The solutions were changed daily to maintain a constant ion concentration, which has been shown to provide the most accurate results.[29] Films were immersed for up to 4 weeks, with samples taken out every week in triplicate and washed with deionized water before being freeze-dried. The samples were analyzed for mass change along with ESEM/EDS and XRD analysis to determine the extent and type of inorganic mineralized phase. The mass gain data is summarized in Figure 2(b). ESEM images and representative EDS spectra are provided in Figures 3 and 4, respectively.

RESULTS AND DISCUSSION

All the polymers in this study were synthesized following a similar procedure. The reactive intermediate, poly(dichlorophosphazene) (**1**), was synthesized via a previously reported route.[18] The chlorine atoms were replaced in two steps to generate the

Table I. Characterization Data for Esterified (2–5) and Deesterified (2a–5a) Polymers

Polymer	^{1}H (ppm)	^{31}P (ppm)	M_w (kDa)	PDI	T_g (°C)	Composition (mol %)	Yield
2[a]	7.00 (4H), 5.80 (1H), 5.14 (2H), 4.42 (2H), 2.94 (3H), 2.30 (2H), 2.16 (5H)	1.85, −2.33	1,928	1.96	−37.8	23% *p*-cresol; 77% *β*-Ala-AE	64%
3[a]	6.79 (4H), 5.70 (1H), 5.07 (2H), 4.30 (2H), 2.91 (3H), 2.21 (5H)	0.47, −2.85, −15.5	3,034	2.00	−30.1	50% *p*-cresol; 50% *β*-Ala-AE	65%
4[a]	7.17 (4H, 6.08 (1H), 5.40 (2H), 4.70 (2H), 2.95 (3H), 2.43 (5H), 1.86 (2H)	2.69, 2.15	1,363	1.27	−58.2	22% *p*-cresol; 78% GABA-AE	43%
5[a]	6.87 (4H), 5.94 (1H), 5.21 (2H), 4.45 (2H), 2.69 (2H), 2.26 (3H), 2.03 (2H), 1.43 (2H)	1.40, −2.39, −15.8	1,557	1.70	−40.2	48% *p*-cresol; 52% GABA-AE	40%
2a[b]	9.03 (1H), 6.99 (4H), 5.88, 5.18, 4.46, 3.40 (2H), 2.99 (1H), 2.32-2.21 (5H)	14.1, 0.811, −7.57	NA[c]	NA[c]	48.2	21% *p*-cresol; 72% *β*-Ala-OH; 7% *β*-Ala-AE	76%
3a[b]	10.92 (1H), 6.85 (4H), 2.93 (2H), 2.18 (5H)	2.85, −3.15, −16.23	NA[c]	NA[c]	56.1	50% *p*-cresol; 50% *β*-Ala-OH	53%
4a[b]	6.98 (4H), 5.87, 5.19, 4.48, 2.72 (2H), 2.11 (2H), 1.78 (3H), 1.54 (2H)	4.07, −1.77	NA[c]	NA[c]	11.7	25% *p*-cresol; 65% GABA-OH; 10% GABA-AE	78%
5a[b]	12.1 (1H), 6.96 (4H), 2.70 (2H), 2.23 (3H), 1.96 (2H), 1.41 (2H)	1.15, −2.87, −16.2	NA[c]	NA[c]	25.8	50% *p*-cresol; 50% GABA-AE	37%

[a] NMR spectra were obtained in chloroform.
[b] NMR spectra were obtained in DMSO-D6.
[c] M_w and PDI could not be obtained due to insufficient solubility in THF. *β*-Ala-AE = *β*-alanine allyl ester, GABA-AE = *γ*-amino butyric acid allyl ester, *β*-Ala-OH = *β*-alanine, GABA-OH = *γ*-amino butyric acid.

final fully substituted materials as shown in Figure 1. The characterization data are provided in Table I. First, poly(dichlorophosphazene) (**1**) was treated with the sodium salt of *p*-cresol to replace either 25% (**2** and **4**) or 50% (**3** and **5**) of the chlorine atoms, followed by the replacement of the remaining halogen by either *β*-Ala-AE (**2** and **3**) or GABA-AE (**4** and **5**). The amino linked group was introduced second in order to limit the total exposure time of the polymer to the hydrogen chloride generated during the substitution reaction. This was done to minimize backbone cleavage.[7] After the macromolecular substitution reactions were complete, the ester units were deprotected by means of the Pd(0)-catalyzed allyl transfer reaction under mild conditions to afford the final polymer with carboxylic acid units. This route allowed the complete de-esterification of polymers **3** and **5,** as confirmed by ^{1}H NMR. However, polymers **2** and **4** precipitated prematurely from solution during the deesterification step, which resulted in their retention of 7 to 10 mol % of their original allyl ester groups. In addition, due to their high acid group content, these polymers were completely water soluble. Because of these two factors, polymers **2a** and **4a** could not be examined for their solid state hydrolysis or mineralization profiles.

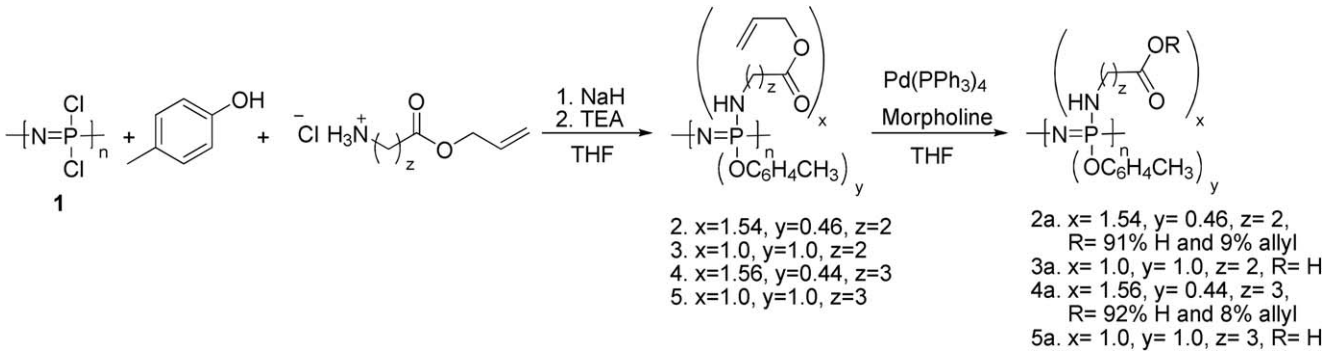

Figure 1. Schematic of the synthesis of β-alanine and γ-amino butyric acid containing polyphosphazenes.

The hydrolysis of solid polymers **3a** and **5a** was carried out over a 6-week period in TRIS buffered saline at pH = 7.35 and at 37°C to simulate physiological conditions. The results are summarized in Figure 2(a). The rates of hydrolysis depended on the nature of the acidic linker group, with the GABA-containing **5a** hydrolyzing at a significantly faster rate (complete degradation within 3 weeks) than the β-Ala-containing **3a** (10% film mass remaining after 6 weeks). This difference may stem from the higher molecular flexibility of GABA groups compared to β-Ala, because of the extra methylene unit in the carbon chain. This allows the carboxylic acid unit easier access to the backbone, and leads to an increased rate of hydrolysis via acidic cleavage. Previous work has shown this mechanism results in the cleavage of the side group from the polymer which results in the formation of a P—OH moiety in its place, which then rearranges to the phosphozane structure which ultimately leads to polymer backbone cleavage.[13,18,30] Additionally, the hydrolytic breakdown is further facilitated by the hydrolytically labile nature of the P—N bond linking the side group to the polymer backbone, which has been shown to be hydrolytically unstable even in the absence of acidic side groups.[13,18,21] These hydrolysis rates are also significantly higher than those measured for the previously published phosphonic acid system,[24] and can be explained by the significantly higher loading of acidic side groups in these polymers.

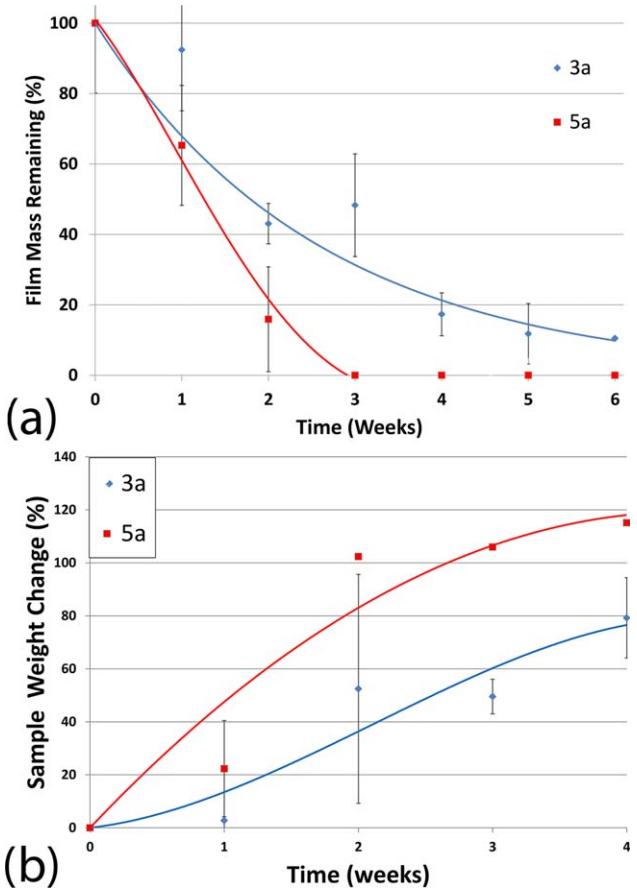

Figure 2. Hydrolysis (a) and mineralization (b) profiles of polymers **3a** and **5a** as a function of the exposure time to SBF. [Color figure can be viewed in the online issue, which is available at wileyonlinelibrary.com.]

The mineralization of polymers **3a** and **5a** was examined in 1.5X SBF at 37°C over a period of 4 weeks, a period chosen to allow sufficient time for mineralization to occur. A dynamic treatment was used, with the solutions changed every 24 h. Calcium phosphate deposition was detected on both polymers, with the total amount dependent on the nature of the acidic side group present (GABA > β-Ala). The data are provided in Figure 2(b). Beginning with the first week of exposure to SBF, both polymers **3a** (15% mass gain) and **5a** (21% mass gain) showed uniform deposition of calcium phosphate across their entire surface, as detected by ESEM (Figure 3) coupled with EDS. However, because phosphorus is also present in the polymer backbone, the calcium phosphate phase could not be identified using the Ca:P ratio calculated using EDS. After 2 weeks exposure to SBF, polymer **3a** (50% mass gain) began to show irregularly shaped structures, while **5a** (105% mass gain) underwent the formation of globular features across its surface. This trend continued into week 3, with a general increase in the density of the mineralized material. This is in contrast to previously developed polyphosphazene samples which showed mostly sporadic deposition of calcium phosphate along their surface which resulted in a maximum of 27% mass gain after immersion in SBF for 4 weeks.[23,31,32]

A major difference between these two systems was evident after 4 weeks of exposure to SBF. At this point, polymer **3a** showed a general expansion of the irregularly shaped surface features which were first seen at week 2. The calcium signal also increased in intensity in the EDS spectra. However, polymer **5a**

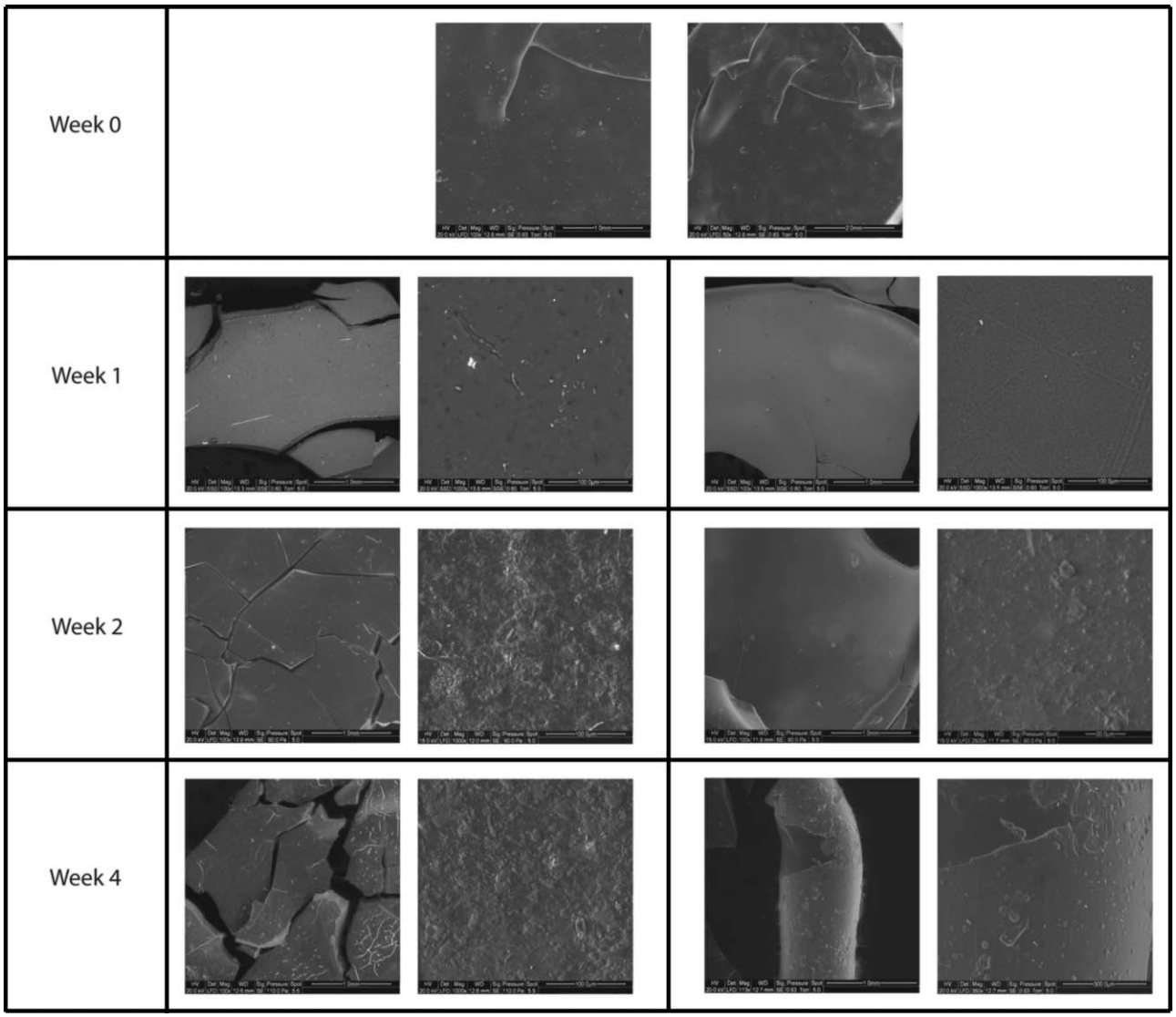

Figure 3. ESEM micrographs of polymers **3a** (left) and **5a** (right) after exposure to SBF.

showed a significantly larger increase in the thickness of the deposited material together with a significant increase in the Ca^{2+} signal, as indicated by EDS (Figure 4). This is also supported by the mass gain data in which polymer **3a** showed a maximum of 79% mass gain, while polymer **5a** showed an increase of 115%. The deposited material had a dense, mainly featureless surface with a thickness that was easily discernible in the ESEM images.

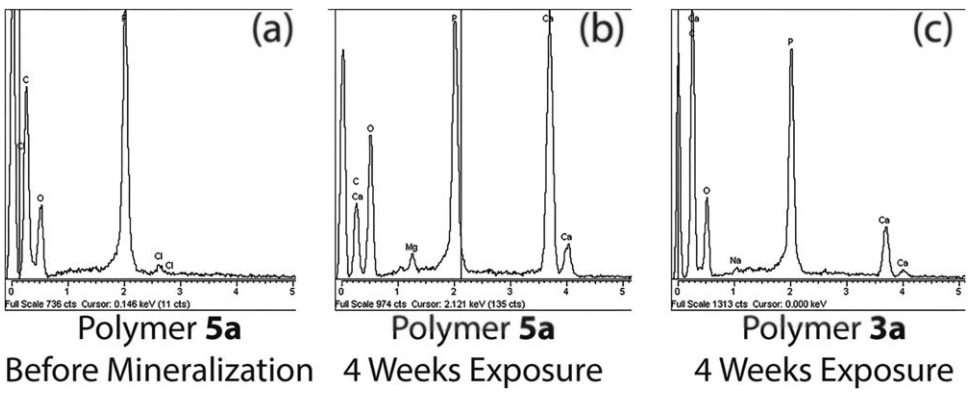

Figure 4. EDS spectra of **5a** before mineralization (a), after 4 weeks exposure to SBF (b), and polymer **3a** after exposure to SBF for 4 weeks (c).

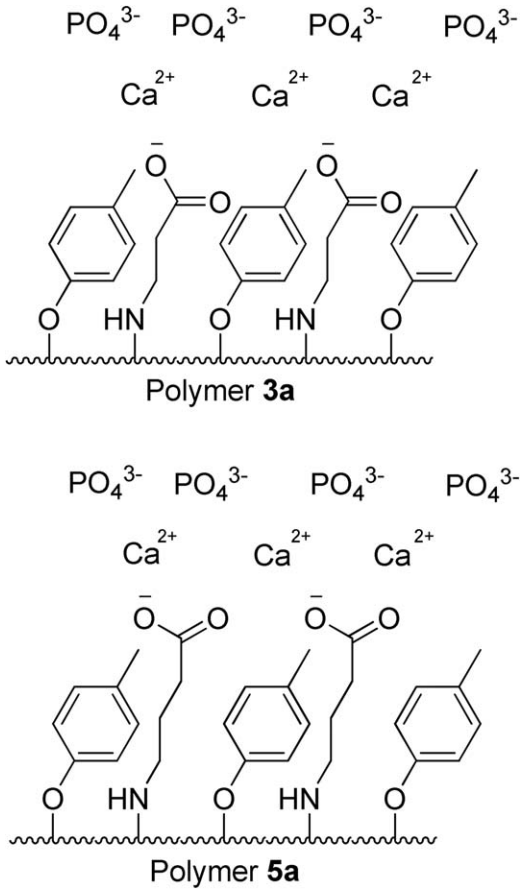

Figure 5. Mineralization mechanism for polymers **3a** and **5a** when immersed in simulated body fluid.

The difference in both the rates and extent of mineralization is attributable to the different types of acidic side groups present on each polymer. The mineralization process begins with the coordination of solution-state Ca^{2+} ions to the carboxylic acid groups.[33] In this case, the extra methylene unit present in the GABA side group, compared to β-Ala, extends the carboxylic acid unit further from the hydrophobic *p*-cresol co-substituents, and this allows easier access to the SBF and facilitates Ca^{2+} coordination. This is illustrated in Figure 5. After binding of the calcium, the now-positively charged surface should attract negatively charged phosphates from solution. This process is then repeated to form the observed inorganic deposits.

To determine the type of calcium phosphate phase deposited on the polymers, the samples were examined using XRD. The XRD patterns obtained for polymers **3a** at weeks 0, 1, 4 and for polymer **5a** at weeks 0 and 4 of mineralization are shown in Figure 6.

Before mineralization, both polymers showed strong broad peaks at $2\theta = 18$–$25°$, centered around $2\theta = 20°$, with polymer **5a** also generating a second peak at $2\theta = 6.8°$. These peaks may be attributed to low level chain packing in these materials, facilitated by hydrogen bonding between the carboxylic acid units. After incubation in SBF, polymer **3a** showed no changes when compared to the original polymer even after 4 weeks immersion [Figure 5(a)]. The absence of a signal from the deposited material is probably due to the smaller amount of calcium phosphate deposited on the polymer.

Similarly, the XRD pattern for polymer **5a** did not show major changes during the first 3 weeks of exposure to SBF. However, after 4 weeks, the XRD spectra underwent a drastic change (Figure 6c). New, broad signals were detected at $2\theta = 26$ and 31–34°, similarly to signals observed in our previous work.[31] By comparing this spectrum with the XRD spectrum of hydroxyapatite, the new signals may be indicative of the 002 and 211/112/300 planes of hydroxyapatite, respectively. The breadth of these peaks is

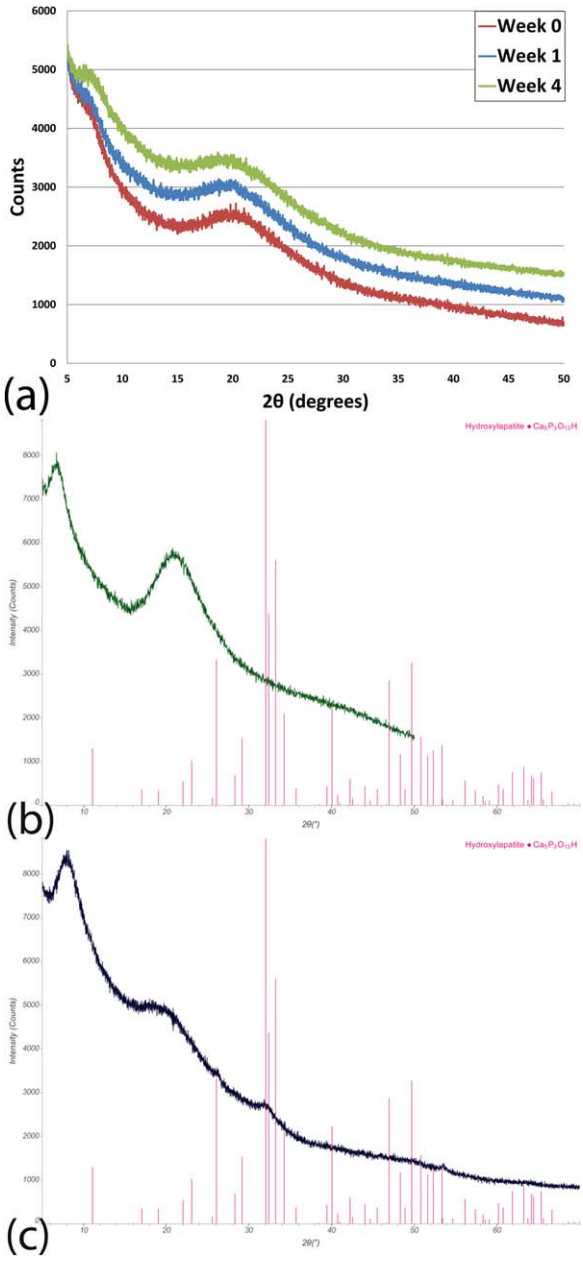

Figure 6. XRD traces of (a) polymer **3a** after exposure to SBF solution for 0 weeks (bottom trace), 1 (middle trace) and 4 (top trace) weeks, (b) polymer **5a** before exposure to SBF and (c) after 4 weeks immersion in SBF overlaid with the trace for hydroxyapatite. [Color figure can be viewed in the online issue, which is available at wileyonlinelibrary.com.]

consistent with previously reported examples of HAp deposited on surfaces[23,34,35] and may correspond to signal broadening reported for amorphous deposited inorganic phosphates.[36]

CONCLUSIONS

Polyphosphazenes with acidic β-alanine and γ-amino butyric acid side groups are capable of nucleating the growth of calcium phosphate during exposure to SBF. Exposure of these polymers to SBF resulted in the growth of inorganic deposits on their surface beginning within the first week. Compared to previously studied polyphosphazenes designed for this application, which showed inhomogeneous deposition of calcium phosphate on their surface even after 4 weeks immersion in SBF, the new polymers undergo a marked increase in both the rate and amount of deposited inorganic phase over their entire surface. Polymer 5a gained a total of 115% mass by week 4, while polymer **3a** showed a lower mass gain of 79%. This can be compared to the maximum 15–30 mass % increase in previously developed systems.[23,31] ESEM and EDS analysis allowed a qualitative identification of the deposited mineral. Thus, both visual appearance and the concurrent increase in the EDS calcium signal, which was uniform and dense across the entire surface of the polymers should make them good candidates for potential bone graft scaffolding materials. XRD analysis supports the conclusion that the deposited material on polymer **5a** is calcium hydroxyapatite. However, due to the breadth of the peaks, it is probably amorphous. This combination of both rapid and extensive calcium phosphate deposition over the entire surface of polymer **5a** makes it the most promising polyphosphazene-based candidate for potential applications as a bone tissue engineering scaffold.

REFERENCES

1. Laurencin, C. T. *Medscape* **2009**. http://emedicine.medscape.com/article/1230616-overview.
2. Nikorn Pothayee, N. P.; Kevin, S.; Suzanne, H.; Abby, M.; Riffle, J. S. *Polym. Prepr.* **2010**, *51*, 92.
3. Betz, R. R. M. D. *Orthopedics* **2002**, *25*, S561.
4. O'Brien, F. *J. Mater. Today* **2011**, *14*, 88.
5. Deng, M.; Nair, L. S.; Nukavarapu, S. P.; Jiang, T.; Kanner, W. A.; Li, X.; Kumbar, S. G.; Weikel, A. L.; Krogman, N. R.; Allcock, H. R.; Laurencin, C. T. *Biomaterials* **2010**, *31*, 4898.
6. Middleton, J. C.; Tipton, A. J. *Biomaterials* **2000**, *21*, 2335.
7. Morozowich, N. L.; Weikel, A. L.; Nichol, J. L.; Chen, C.; Nair, L. S.; Laurencin, C. T.; Allcock, H. R. *Macromolecules* **2011**, *44*, 1355.
8. Fu, K.; Pack, D. W.; Klibanov, A. M.; Langer, R. *Pharm. Res.* **2000**, *17*, 100.
9. Francolini, I.; Donelli, G.; Stoodley, P. *Rev. Environ. Sci. Bio/Technol.* **2003**, *2*, 307.
10. Pramanik, N.; Mishra, D.; Banerjee, I.; Maiti, T. K.; Bhargave, P.; Pramanik, P. *Int. J. Biomater.* **2009**, *2009*, 8.
11. Liu, X.; Ma, P. X. *Ann. Biomed. Eng.* **2004**, *32*, 477.
12. Deng, M.; Nair, L. S.; Krogman, N. R.; Allcock, H. R.; Laurencin, C. T. In Polyphosphazenes for Biomedical Applications; Andrianov, A. K., Ed.; Wiley: Hoboken, NJ, **2009**; p 139.
13. Allcock, H. R.; Morozowich, N. L. *Polym. Chem.* **2012**, *3*, 578.
14. Choong, C.; Yuan, S.; Thian, E. S.; Oyane, A.; Triffitt, J. *J. Biomed. Mater. Res. A* **2012**, *100A*, 353.
15. Gemeinhart, R. A.; Bare, C. M.; Haasch, R. T.; Gemeingart, E. J. *J. Biomed. Mater. Res. A* **2006**, *78*, 433.
16. Phadke, A.; Zhang, C.; Hwang, Y.-S.; Vecchio, K.; Varghese, S. *Biomacromolecules* **2010**, *11*, 2060.
17. Allcock, H. R. *J. Inorg. Organometallic Polym. Mater.* **2006**, *16*, 277.
18. Allcock, H. R. Chemistry and Applications of Polyphosphazenes; Wiley: Hoboken, NJ, **2003**.
19. Sethuraman, S.; Nair, L. S.; El-Amin, S.; Farrar, R.; Nguyen, N. M.-T.; Singh, A.; Allcock, H. R.; Greish, Y. E.; Brown, P. W.; Laurencin, C. T. *J. Biomed. Mater. Res. A* **2006**, *77*, 679.
20. Sethuraman, S.; Nair, L. S.; El-Amin, S.; Nguyen, M.-T.; Singh, A.; Greish, Y. E.; Allcock, H. R.; Brown, P. W.; Laurencin, C. T. *J. Biomater. Sci. Polym. Ed.* **2011**, *22*, 733.
21. Allcock, H. R.; Pucher, S. R.; Scopelianos, A. G. *Macromolecules* **1994**, *27*, 1071.
22. Kumbar, S. G.; Bhattacharyya, S.; Nukavarapu, S. P.; Khan, Y. M.; Nair, L. S.; Laurencin, C. T. *J. Inorg. Organometall. Polym. Mater.* **2006**, *16*, 365.
23. Morozowich, N. L.; Lerach, J. O.; Modzelewski, T.; Jackson, L.; Winograd, N.; Allcock, H. R. *RSC Adv.* **2014**, *4*, 19680.
24. Morozowich, N. L.; Modzelewski, T.; Allcock, H. R. *Macromolecules* **2012**, *45*, 7684.
25. Nair, L. S.; Lee, D. A.; Bender, J. D.; Barrett, E. W.; Greish, Y. E.; Brown, P. W.; Allcock, H. R.; Laurencin, C. T. *J. Biomed. Mater. Res. A* **2006**, *76*, 206.
26. Tanahashi, M.; Yao, T.; Kokubo, T.; Minoda, M.; Miyamoto, T.; Nakamura, T.; Yamamuro, T. *J. Am. Ceram. Soc.* **1994**, *77*, 2805.
27. Tanahashi, M.; Yao, T.; Kokubo, T.; Minoda, M.; Miyamato, T.; Nakamura, T.; Yamamuro, T. *J. Am. Ceram. Soc.* **1994**, *77*, 2805.
28. Abe, Y.; Kawashita, M.; Kokubo, T.; Nakamura, T. *J. Seram. Soc. Jpn.* **2001**, *109*, 106.
29. Zimmerman, K. A.; LeBlanc, J. M.; Sheets, K. T.; Fox, R. W.; Gatenholm, P. *Mater. Sci. Eng. C* **2011**, *31*, 43.
30. Andrianov, A.; Marin, A.; Chen, J. *Biomacromolecules* **2006**, *7*, 394.
31. Morozowich, N. L.; Nichol, J. L.; Allcock, H. R. *Chem. Mater.* **2012**, *24*, 3500.
32. Morozowich, N. L.; Nichol, J. L.; Mondschein, R. J.; Allcock, H. R. *Polym. Chem.* **2012**, *3*, 778.
33. Oyane, A.; Uchida, M.; Choong, C.; Triffitt, J.; Jones, J.; Ito, A. *Biomaterials* **2005**, *26*, 2407.
34. Zhang, R.; Ma, P. X. *J. Biomed. Mater. Res.* **1998**, *45*, 285.
35. Costa, D. O.; Allo, B. A.; Klassen, R.; Hutter, J. L.; Dixon, S. J.; Rizkalla, A. S. *Langmuir* **2012**, *28*, 3871.
36. Bushroa, A. R.; Rahbari, R. G.; Masjuki, H. H.; Muhamad, M. R. *Vacuum* **2012**, *86*, 1107.